

# SYNTHESIS AND MAGNETOCALORIC EFFECT OF Co-SUBSTITUTED $ZnFe_2O_4$ NANOPARTICLES WITH POLYOL METHOD

## POLIOLSKA SINTEZA IN MAGNETOKALORIČNI UČINEK S KOBALTOM OBOGATENIH $ZnFe_2O_4$ NANODELCEV

Haitao Zhao\*, Xuehan Li, Hui Zhao, Yulian Wang

School of Materials Science and Engineering, Shenyang Ligong University, No. 6 Nanping Middle Road, Hunnan New District, Liaoning Province, 110 159 Shenyang, China

Prejem rokopisa – received: 2019-12-10; sprejem za objavo – accepted for publication: 2020-05-22

doi:10.17222/mit.2019.293

Spinel  $Co_xZn_{1-x}Fe_2O_4$  ( $x = 0, 0.2, 0.4, 0.6, 0.8$ ) nanoparticles with sodium citrate as the surfactant were fabricated using the polyol process. The Co-substituted effect on the structure, morphology, magnetic and magnetocaloric properties of  $ZnFe_2O_4$  ferrites were investigated with X-ray diffraction (XRD), transmission electron microscopy (TEM) and vibrating-sample magnetometry (VSM). The results indicate that the Co-substituted  $ZnFe_2O_4$  ferrites have a pure cubic spinel structure with a particle size of 6–9 nm. The  $Co_xZn_{1-x}Fe_2O_4$  particles exhibit ferromagnetic behavior with a small hysteresis at room temperature. An increase in the Co-content leads to an increase in the saturation-magnetization value (Ms). The Ms value is drastically raised to 44.26 emu/g. The temperature of  $Co_xZn_{1-x}Fe_2O_4$  in an alternating magnetic field is also increased with an increase in  $x$ . The final temperature of  $Co_{0.8}Zn_{0.2}Fe_2O_4$  can reach 52 °C when the ferrite is placed in a magnetic field for 600 s, and the magnetocaloric effect is very significant.

Keywords: Co-substituted  $ZnFe_2O_4$ , nanostructures, polyol method, magnetocaloric effect

Avtorji članka opisujejo izdelavo špinelnih  $Co_xZn_{1-x}Fe_2O_4$  ( $x = 0, 0.2, 0.4, 0.6, 0.8$ ) nanodelcev s polioličnim postopkom, pri katerem je bil uporabljen natrijev citrat kot površinsko aktivna snov. Avtorji so raziskovali vpliv nadomeščanja (delne zamenjave) cinkovih ionov s kobaltom na strukturo, morfologijo, magnetne in magnetokalorične lastnosti  $ZnFe_2O_4$  feritov. Raziskave so izvajali z opazovanjem pod presevnim elektronskim mikroskopom (TEM), z rentgensko difrakcijo (XRD) in vibracijsko magnetometrijo vzorcev (VSM). Rezultati raziskav kažejo, da imajo s kobaltom obogateni  $ZnFe_2O_4$  feriti čisto kubično špinelno strukturo z delci velikosti od 6 nm do 9 nm. Nanodelci  $Co_xZn_{1-x}Fe_2O_4$  imajo ferimagnetne lastnosti z majhno histerezo pri sobni temperaturi. Povečanje vsebnosti Co poviša vrednost magnetizacije pri nasičenju (Ms). Tako se Ms vrednost pri  $x = 0.8$  drastično poveča na 44,26 emu/g. Temperatura  $Co_xZn_{1-x}Fe_2O_4$  v izmeničnem magnetnem polju prav tako narašča z naraščajočo vrednostjo  $x$ . Najvišjo temperaturo (52 °C) in tako velik magnetokalorični učinek so dosegli, ko so  $Co_{0.8}Zn_{0.2}Fe_2O_4$  ferit izpostavili za 600 s v izmenično (50 Hz) magnetno polje.

Ključne besede: s kobaltom obogateni  $ZnFe_2O_4$ , nanostrukture, poliolična metoda, magneto-kalorični učinek

## 1 INTRODUCTION

In recent years, nanostructured magnetic materials with a well-defined morphology and size distribution have been considered very attractive due to their microstructure-dependent physical and chemical properties. They have been studied extensively with respect to a variety of applications, including magnetic storage,<sup>1</sup> resonance imaging,<sup>2</sup> targeted drug delivery,<sup>3</sup> hyperthermia<sup>4</sup> and so on. Therefore, various research groups have proposed different techniques to synthesize nanostructured magnetic materials like the hydrothermal method, co-precipitation, thermal decomposition and the polyol method.<sup>5–8</sup> However, among the above methods, the polyol method has been of significant interest in fabricating the homogeneous nanostructured magnetic powders because of its inexpensive precursors, short preparation time, rather mild conditions without the need for further

calcination and relatively simple manipulation.<sup>9–11</sup> In this method, a high-boiling-point solvent is used as the solvent as well as the reducing agent of the metallic ions under reflux conditions, creating the product's own hydrophilic properties, therefore providing the potential for application in the biomedical field.

Among these magnetic materials, spinel-type ferrites have shown a growing interest in recent years due to their specific magnetic and electrical properties, such as their chemical stability, low eddy-current loss and high resistivity.<sup>12–14</sup> Herein, the Co-Zn mixed ferrite has attracted considerable attention due to the diverse properties of  $ZnFe_2O_4$  and  $CoFe_2O_4$ . The crystal structure of spinel ferrites can generally be described with formula  $AB_2O_4$  where A and B denote divalent and trivalent cations, respectively.<sup>15</sup> The cation distribution between both sites is described by the inversion parameter  $v$ .<sup>16</sup> Zinc ferrite and cobalt ferrite represent two members of the family of magnetic spinel-type oxides, exhibiting the typically normal and inverse spinel ferrites, respectively.

\*Corresponding author's e-mail:  
zht95711@163.com (Haitao Zhao)

Singh<sup>17</sup> et al. prepared zinc-substituted cobalt ferrites via the reverse-micelle technique and investigated the structural, magnetic, optical and catalytic properties of the products.<sup>17</sup> Jnaneshwara et al. also prepared Co-Zn ferrite powders using the solution-combustion method, and studied the magnetic and dielectric properties of the samples. The samples were quite useful for the fabrication of nanoelectronic devices.<sup>18</sup> Manikandan and co-workers reported on the synthesis of Zn<sub>1-x</sub>Co<sub>x</sub>Fe<sub>2</sub>O<sub>4</sub> nanoparticles with various particle sizes, achieved with the microwave-combustion method using urea as a fuel. The relatively high Ms of the samples suggests that this method is suitable for preparing high-quality nanocrystalline magnetic ferrites for practical applications.<sup>19</sup>

However, to the best of our knowledge, no study on the magnetocaloric effect of monodisperse Co-substituted ZnFe<sub>2</sub>O<sub>4</sub> synthesized via the polyol process has been reported until now. The addition of Co<sup>2+</sup> ions into zinc ferrite affects the lattice parameter, the crystallite size and the magnetic properties. In this study, Co-substituted ZnFe<sub>2</sub>O<sub>4</sub> nanoparticles obtained with the polyol method using sodium citrate as the surfactant are synthesized. The size distribution, particle morphology and shape of the products are controlled. Therefore, the objective of our present work is to study the magnetocaloric effect of the Co-Zn ferrites and evaluate their structural, morphological and magnetic properties.

## 2 EXPERIMENTAL PART

Iron acetylacetonate (Fe(acac)<sub>3</sub>), zinc acetylacetonate (Zn(acac)<sub>2</sub>), cobalt acetylacetonate (Co(acac)<sub>2</sub>), sodium citrate, triethylene glycol (TEG) were purchased from Sinopharm Chemical Reagent Co., Ltd and all the reaction reagents were of the analytical grade and used as received.

Nanocrystalline powders of Co-substituted ZnFe<sub>2</sub>O<sub>4</sub> ferrites with nominal compositions Co<sub>x</sub>Zn<sub>1-x</sub>Fe<sub>2</sub>O<sub>4</sub> ( $x = 0, 0.2, 0.4, 0.6, 0.8$ ) were synthesized via the polyol technique. A mixture of the precursor with sodium citrate and 50-mL TEG was directly put into a three-neck round-bottomed flask, equipped with a condenser, magnetic stirrer and heating system. The reaction system was heated to 80 °C and maintained for 10 min. The temperature was gradually increased to 190 °C and also maintained for 10 min; then the solution was refluxed at 266 °C for 30 min before cooling it down to room temperature. The obtained black mixture was collected, using a magnet and washed with ethanol three times using centrifugation. This was followed by 12-h drying in a vacuum oven to obtain Co-Zn ferrite nanoparticles. All the synthesis processes were carried out in an argon atmosphere.

The phase structure of the synthesized product was confirmed with X-ray diffraction (PW-3040, Holland, PANalytical B.V. Company) using Cu-K<sub>α</sub> radiation ( $\lambda = 0.15418$  nm) with a scanning rate of 0.02 °/s in a  $2\theta$

range of 20–70°. The morphology and size of the products were observed using transmission electron microscopy (TEM, Philips EM 420). Fourier transform infrared (FTIR) spectroscopic data was taken to reveal the surface modification in a range of 4000–500 cm<sup>-1</sup> using KBr-pressed pellets. The magnetic properties of products were measured using a vibrating-sample magnetometer (VSM-220) in an external field of up to 15 kOe at room temperature. The magnetocaloric effect was measured using a generator which can create an alternating magnetic field with a frequency of 50 kHz. Samples were dispersed in 1-mL water and kept in a round-bottom glass holder. The temperature increase of the suspension was obtained with an alcohol thermometer. The measured period was 600 s.

## 3 RESULTS

**Table 1:** Characteristic parameters of as-synthesized Co<sub>x</sub>Zn<sub>1-x</sub>Fe<sub>2</sub>O<sub>4</sub> ferrites

| Co-content | Formula  | <i>a</i> (nm) | <i>D</i> <sub>TEM</sub> (nm) |
|------------|--|---------------|------------------------------|
| 0.0        | ZnFe <sub>2</sub> O <sub>4</sub>                                   | 0.8439        | 5.21                         |
| 0.2        | Co <sub>0.2</sub> Zn <sub>0.8</sub> Fe <sub>2</sub> O <sub>4</sub> | 0.8428        | 5.23                         |
| 0.4        | Co <sub>0.4</sub> Zn <sub>0.6</sub> Fe <sub>2</sub> O <sub>4</sub> | 0.8419        | 5.55                         |
| 0.6        | Co <sub>0.6</sub> Zn <sub>0.4</sub> Fe <sub>2</sub> O <sub>4</sub> | 0.8411        | 5.75                         |
| 0.8        | Co <sub>0.8</sub> Zn <sub>0.2</sub> Fe <sub>2</sub> O <sub>4</sub> | 0.8403        | 5.80                         |

**Table 2:** Magnetic parameters of as-synthesized Co<sub>x</sub>Zn<sub>1-x</sub>Fe<sub>2</sub>O<sub>4</sub> ferrites

| Formula  | <i>M</i> <sub>s</sub> (emu/g) | <i>M</i> <sub>r</sub> (emu/g) | <i>H</i> <sub>c</sub> (Oe) |
|--|-------------------------------|-------------------------------|----------------------------|
| ZnFe <sub>2</sub> O <sub>4</sub>                                   | 35.09                         | 0.63                          | 52.38                      |
| Co <sub>0.2</sub> Zn <sub>0.8</sub> Fe <sub>2</sub> O <sub>4</sub> | 38.51                         | 0.73                          | 56.82                      |
| Co <sub>0.4</sub> Zn <sub>0.6</sub> Fe <sub>2</sub> O <sub>4</sub> | 38.48                         | 1.3                           | 71.15                      |
| Co <sub>0.6</sub> Zn <sub>0.4</sub> Fe <sub>2</sub> O <sub>4</sub> | 44.24                         | 1.49                          | 84.5                       |
| Co <sub>0.8</sub> Zn <sub>0.2</sub> Fe <sub>2</sub> O <sub>4</sub> | 44.26                         | 2.02                          | 98.83                      |

## 4 DISCUSSION

**Figure 1** presents the XRD patterns obtained at different Co-contents. It can be observed that the diffraction peaks of each sample are well indexed to the (220), (311), (400), (422), (511) and (440) planes of the spinel structure, matching well with the standard powder diffraction data (PDF file No.: 00-022-1012). There are no detected diffraction peaks of any other phase, which indicates that high-purity products are obtained. The broad shape and low intensity of the diffraction peaks indicate a small size of the nanocrystals<sup>20</sup>. Lattice parameters are calculated according to Equation (1)<sup>21</sup> and the results are summarized in **Table 1**.

$$a = \frac{\lambda \sqrt{(h^2 + k^2 + l^2)}}{2 \sin \theta} \quad (1)$$

Here,  $\lambda$  is the wavelength of the X-ray radiation, 0.154178 nm;  $2\theta$  is the position of the diffraction peak and (hkl) are the corresponding Miller indices.

In **Table 1**, it can be found that with the Co-content increasing from 0 to 0.8, the lattice parameters of the ferrites decrease from 0.8439 nm to 0.8403 nm. The lattice constant variation trend may be related to the fact that Zn ions (0.074 nm) were replaced by Co ions with a slightly smaller ionic radius (0.072 nm). So, it is believed that a higher degree of Co substitution leads to a smaller lattice constant. A. V. Raut et al.<sup>22</sup> also reached a similar conclusion.

**Figure 2** illustrates the TEM images and corresponding particle-size histograms of  $\text{Co}_x\text{Zn}_{1-x}\text{Fe}_2\text{O}_4$  ( $x = 0, 0.2, 0.4, 0.6, 0.8$ ) ferrites. The TEM analysis reveals that the as-synthesized products are composed of monodisperse spherical nanoparticles with the average size about 6 nm. From the corresponding particle-size histograms, it can be observed that the size distribution for all the samples is narrower and the dimensions of the samples are less than 10 nm. This is because the primary crystals tend to be fully capped by the layer of surfactant in a short time, and the grain growth as well as aggregation process are inhibited, allowing one to obtain monodisperse and small-sized nanoparticles.<sup>23</sup> The particle sizes estimated from the obtained TEM images of these samples are also listed in **Table 1** along with the other parameters.

**Figure 3** shows the FTIR spectra of  $\text{Co}_x\text{Zn}_{1-x}\text{Fe}_2\text{O}_4$  ferrites with different Co-contents. There is a broad peak at around  $3422\text{ cm}^{-1}$  that may be due to the hydrogen-bonded O–H stretching vibration arising from the surface hydroxyl groups on nanoparticles. The bands at  $1599\text{ cm}^{-1}$  and  $1389\text{ cm}^{-1}$  can be attributed to the characteristic band of  $-\text{COOM}$ ,<sup>24</sup> which confirms that sodium citrate is bound to the surfaces of ferrite nanocrystals. In particular, the main broad metal–oxygen bands are seen in the FT-IR spectra of all the Co–Zn ferrites. The band observed at around  $580\text{ cm}^{-1}$  for all the samples can be assigned to the intrinsic vibrations of the tetrahedral site,  $\nu_1$ . This confirms the spinel structure of the prepared ferrites.<sup>25</sup> At a closer look at the  $\nu_1$  band position, it can be observed that the  $\nu_1$  band shifts gradually from  $580\text{ cm}^{-1}$

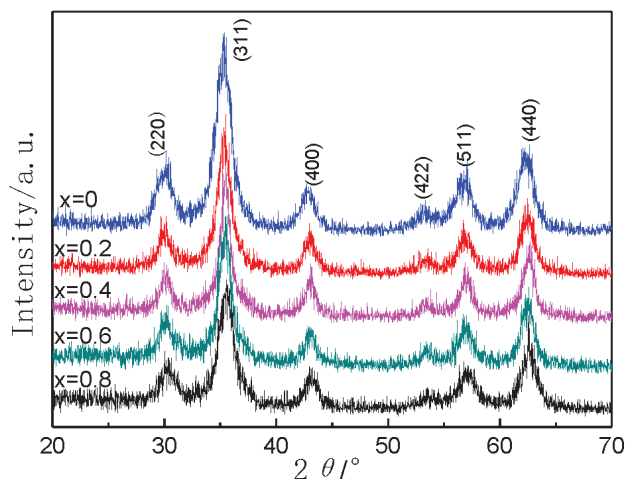


**Figure 1:** XRD patterns of  $\text{Co}_x\text{Zn}_{1-x}\text{Fe}_2\text{O}_4$  ferrites

for  $x = 0$  to  $589\text{ cm}^{-1}$  for  $x = 0.8$  with the increasing Co-content. This can be correlated to the weakening of the metal–oxygen bonds at the tetrahedral sites due to the transition between the extent of normal spinel and inverse structure.<sup>26</sup>

The magnetic-hysteresis loops for the Co–Zn ferrite nanoparticles with different concentrations of  $\text{Co}^{2+}$  ions were investigated at 298 K using VSM and applying an external magnetic field of  $\pm 15\text{ kOe}$ , as shown in **Figure 4**. The main magnetic parameters including saturation magnetization ( $M_s$ ), remanence magnetization ( $M_r$ ) and coercivity ( $H_c$ ) of the  $\text{Co}_x\text{Zn}_{1-x}\text{Fe}_2\text{O}_4$  ferrites are listed in **Table 2**. It is observed that all the samples exhibit a

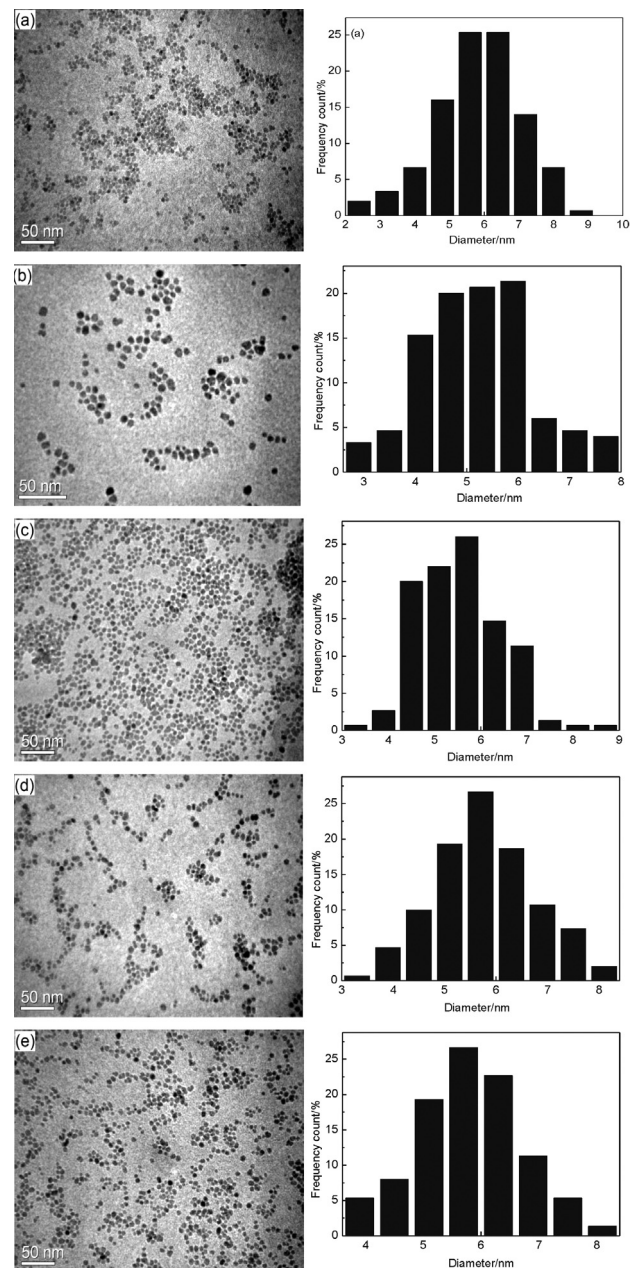


**Figure 2:** TEM images and corresponding particle-size histograms of  $\text{Co}_x\text{Zn}_{1-x}\text{Fe}_2\text{O}_4$  ferrites

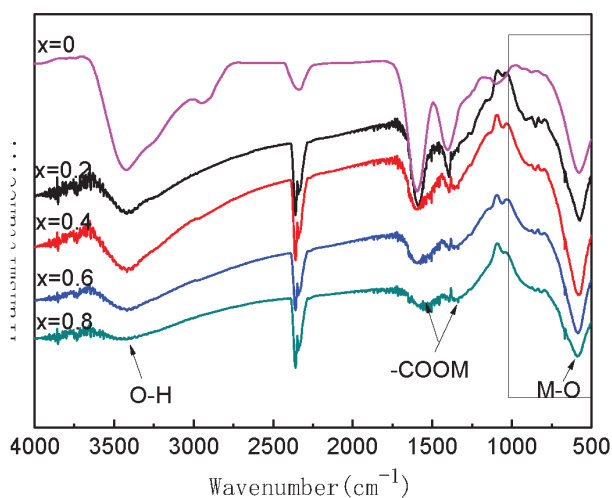


Figure 3: FTIR-spectra of Co<sub>x</sub>Zn<sub>1-x</sub>Fe<sub>2</sub>O<sub>4</sub> ferrites

small hysteresis, indicating that the synthesized Co<sub>x</sub>Zn<sub>1-x</sub>Fe<sub>2</sub>O<sub>4</sub> nanocrystals show ferromagnetic behavior at room temperature. In the spinel ferrites, the magnetic order mostly occurred due to the superexchange interactions between the metal ions of two sublattices, the tetrahedral lattice (A) and octahedral position (B)<sup>27</sup>. The distribution of ions in the lattice includes non-magnetic Zn<sup>2+</sup> ions found in the A sites, magnetic Co<sup>2+</sup> ions that prefer the B sites and Fe<sup>3+</sup> ions occupying both positions A and B. It is commonly believed that ZnFe<sub>2</sub>O<sub>4</sub> should exhibit antiferromagnetic behavior; however, when the grain size is reduced to nanosize, the zinc ferrite presents

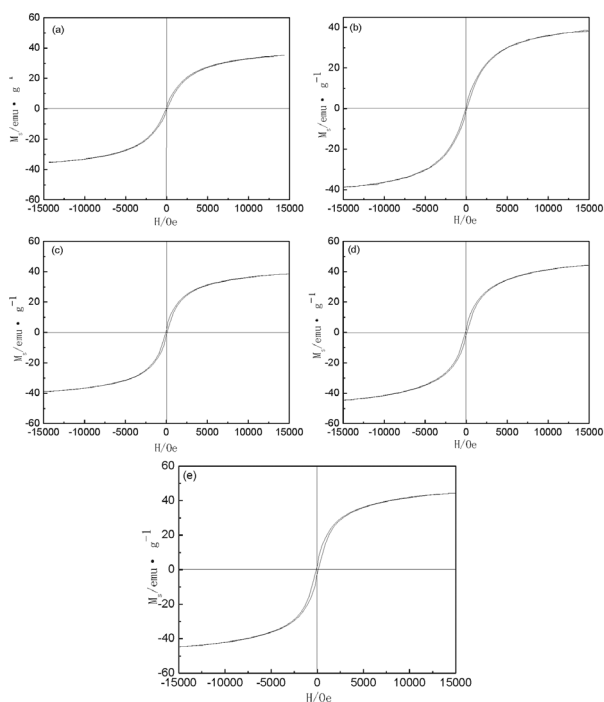


Figure 4: Hysteresis loops of Co<sub>x</sub>Zn<sub>1-x</sub>Fe<sub>2</sub>O<sub>4</sub> ferrite nanocrystals (at 298 K): a) x = 0, b) x = 0.2, c) x = 0.4, d) x = 0.6, e) x = 0.8

a ferromagnetic behavior. The reason for this phenomenon was explained in our previous report. It is also observed that the saturation magnetization increases with the increasing Co<sup>2+</sup> ion concentration (Table 2). The M<sub>s</sub> changes from 35.09 emu/g for x = 0 to 44.26 emu/g for x = 0.8. The increase in the saturation magnetization is directly related to the substitution of Zn<sup>2+</sup> by Co<sup>2+</sup>. According to Neel’s two-sublattice model, the magnetic moment is expressed:

$$M = M_B - M_A \tag{2}$$

where M<sub>A</sub> and M<sub>B</sub> are the magnetizations of the A and B sublattices, respectively.

In ZnFe<sub>2</sub>O<sub>4</sub>, the Fe<sup>3+</sup> ions in the tetrahedral and octahedral positions have equal and opposite magnetic moments, so they are compensated. With the Co<sup>2+</sup> ion substitution, they have the tendency to occupy octahedral sites and some of the Fe<sup>3+</sup> ions get transferred to the tetrahedral site. In this case, the magnetic moments of the Fe<sup>3+</sup> ions in the two lattices (A and B) no longer compensate, which makes the A–B interaction stronger and causes an increase in the M<sub>s</sub> of the Co<sub>x</sub>Zn<sub>1-x</sub>Fe<sub>2</sub>O<sub>4</sub> nanocrystals. The behavior of coercivity in the Co<sub>x</sub>Zn<sub>1-x</sub>Fe<sub>2</sub>O<sub>4</sub> spinel ferrite system may be associated with the anisotropy of the cobalt ions at the octahedral site due to its important spin-orbit coupling. With the increasing Co-content, the magneto-crystalline anisotropy increases, leading to a decrease of the domain-wall energy, resulting in a larger coercive force.<sup>27</sup>

Figure 5 shows the heating curves of Co<sub>x</sub>Zn<sub>1-x</sub>Fe<sub>2</sub>O<sub>4</sub> nanoparticles under 50 kHz. It is seen from the diagram that the final temperature under the alternating magnetic field increases with the increasing Co-content. The final temperature can reach (39, 42, 47, 49 and 52) °C when x = (0, 0.2, 0.4, 0.6 and 0.8). Co<sub>x</sub>Zn<sub>1-x</sub>Fe<sub>2</sub>O<sub>4</sub> nanoparticles exhibit energy conversion under the action of an alternating magnetic field, which converts some electromagnetic energy into the thermal energy and increases their temperature. The magnetic loss mainly includes the eddy-current loss, hysteresis loss and residual loss, but usually the eddy-current loss and residual loss can be ig-

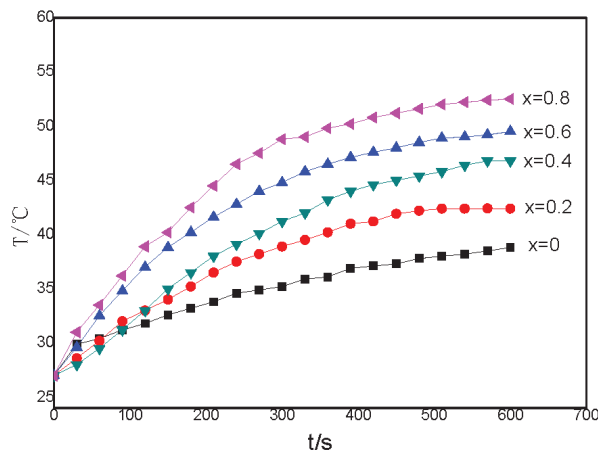


Figure 5: Heating curves of Co<sub>x</sub>Zn<sub>1-x</sub>Fe<sub>2</sub>O<sub>4</sub> ferrites

nored. Therefore, the hysteresis loss of a sample is the main one. The hysteresis loss is due to the irreversible magnetic field generated by the irreversible domain-wall displacement and the moving of the magnetization vector. In the case of a certain magnetic field, the hysteresis loss can be approximately expressed with the product of the saturation magnetization and coercivity. The results show that the higher the hysteresis loss, the more significant is the magnetocaloric effect. With the increase in  $x$ , the saturation magnetization and coercivity of the products increase. Therefore, the temperature of the product in the alternating magnetic field is also increased with the increase in  $x$ . At  $x = 0.8$ , the final temperature can reach 52 °C when the ferrite is placed in the magnetic field for 600 s, and the magnetocaloric effect is very significant.

## 5 CONCLUSIONS

Monodisperse Co-substituted ZnFe<sub>2</sub>O<sub>4</sub> ferrite nanoparticles with the average size in a range of 6–9 nm were synthesized with the one-step, facile and inexpensive polyol method. The addition of Co<sup>2+</sup> ions into zinc ferrite affects the lattice parameter and crystallite size. With the Co-content increasing from 0 to 0.8, the lattice parameters of the ferrites decrease from 0.8439 nm to 0.8403 nm. All the samples exhibit a small hysteresis, indicating that the Co-substituted nanoparticles exhibit ferromagnetic behavior at room temperature. The saturation magnetization increases with the increasing of Co<sup>2+</sup> ion concentration. The Ms value changes from 35.09 emu/g for  $x = 0$  to 44.23 emu/g for  $x = 0.8$ . The final temperature under an alternating magnetic field increases with the increasing Co-content. The final temperature can reach 39, 42, 47, 49 and 52 °C when  $x = (0, 0.2, 0.4, 0.6$  and  $0.8)$ , showing that the magnetocaloric effect of Co <sub>$x$</sub> Zn <sub>$1-x$</sub> Fe<sub>2</sub>O<sub>4</sub> nanoparticles is very significant.

## Acknowledgment

This work was financially supported by the National Natural Science Foundation of China (51303108) and Equipment Pre-Research Project (61409230605).

## 6 REFERENCES

- S. Saranya, B. Saravanan, Optimal size allocation of superconducting magnetic energy storage system based unit commitment, *Journal of Energy Storage*, 20 (2018), 173–189, doi:10.1016/j.est.2018.09.011
- P. Hernandez-Gomez, M. A. Valente, M. P. Graça, Synthesis, structural characterization and broadband ferromagnetic resonance in Li ferrite nanoparticles, *Journal of Alloys and Compounds*, 765 (2018), 186–192, doi:10.1016/j.jallcom.2018.06.172
- G. S. Wang, D. X. Zhao, Y. X. Ma, Synthesis and characterization of polymer-coated manganese ferrite nanoparticles as controlled drug delivery, *Applied Surface Science*, 428 (2018), 258–263, doi:10.1016/j.apsusc.2017.09.096
- G. Hamid, A. Majid, O. Neriman, Hyperthermia application of zinc doped nickel ferrite nanoparticles, *Journal of Physics and Chemistry of Solids*, 111 (2017), 464–472, doi:10.1016/j.jpcs.2017.08.018
- J. C. Fariñas, R. Moreno, A. Pérez, Microwave-assisted solution synthesis, microwave sintering and magnetic properties of cobalt ferrite, *Journal of the European Ceramic Society*, 38 (2017), 2360–2368, doi:10.1016/j.jeurceramsoc.2017.12.052
- T. S. Kuru, M. Kuru, S. Bag, Structural, dielectric and humidity properties of Al-Ni-Zn ferrite prepared by co-precipitation method, *Journal of Alloys and Compounds*, 735 (2018), 483–490, doi:10.1016/j.jallcom.2018.04.255
- G. Singh, S. Chandra, Electrochemical performance of MnFe<sub>2</sub>O<sub>4</sub> nano-ferrites synthesized using thermal decomposition method, *International Journal of Hydrogen Energy*, 43 (2018), 4058–4066, doi:10.1016/j.ijhydene.2017.08.181
- J. H. Peng, Z. W. Peng, Z. P. Zhua, Achieving ultra-high electromagnetic wave absorbing by anchoring Co<sub>0.33</sub>Ni<sub>0.33</sub>Mn<sub>0.33</sub>Fe<sub>2</sub>O<sub>4</sub> nanoparticles on graphene sheets using microwave assisted polyol method, *Ceramics International*, 44 (2018), 21015–21026, doi:10.1016/j.ceramint.2018.08.137
- L. V. Leonel, B. S. Barbosa, R. Miquita, Facile polyol synthesis of ultrasmall water-soluble cobalt ferrite nanoparticles, *Solid State Sciences*, 86 (2018), 45–52, doi:10.1016/j.solidstatesciences.2018.09.011
- J. Töpfer, A. Angermann, Nanocrystalline magnetite and Mn-Zn ferrite particles via the polyol process: Synthesis and magnetic properties, *Materials Chemistry and Physics*, 129 (2011), 337–342, doi:10.1016/j.matchemphys.2011.04.025
- A. Mohamed, S. R. Torati, B. P. Rao, Size controlled sonochemical synthesis of highly crystalline superparamagnetic Mn-Zn ferrite nanoparticles in aqueous medium, *Journal of Alloys and Compounds*, 644 (2015), 774–782, doi:10.1016/j.jallcom.2015.05.101
- A. M. Ibrahim, M. M. Abd El-Latif, M. M. Mahmoud, Synthesis and characterization of nano-sized cobalt ferrite prepared via polyol method using conventional and microwave heating techniques, *Journal of Alloys and Compounds*, 506 (2010), 201–204, doi:10.1016/j.jallcom.2010.06.177
- M. Gunay, H. Kavas, A. Baykal, Simple polyol route to synthesize heptanoic acid coated magnetite (Fe<sub>3</sub>O<sub>4</sub>) nanoparticles, *Materials Research Bulletin*, 48 (2013), 1296–1303, doi:10.1016/j.materresbull.2012.12.028
- Z. Beji, L. S. Smiri, M. J. Vaulay, Nanocrystalline Ni<sub>0.8</sub>Zn<sub>0.2</sub>Fe<sub>2</sub>O<sub>4</sub> films prepared by spray deposition from polyol-mediated sol: Microstructural and magnetic characterization, *Thin Solid Films*, 518 (2010), 2592–2598, doi:10.1016/j.tsf.2009.07.188
- J. Jiang, L. C. Li, Synthesis of sphere-like Co<sub>3</sub>O<sub>4</sub> nanocrystals via a simple polyol route, *Materials Letters*, 61 (2007), 4894–4896, doi:10.1016/j.matlet.2007.03.067
- J. Topfer, A. Angermann, Nanocrystalline magnetite and Mn-Zn ferrite particles via the polyol process: Synthesis and magnetic properties, *Materials Chemistry and Physics*, 129 (2011), 337–342, doi:10.1016/j.matchemphys.2011.04.025
- C. Singh, S. Jauhar, V. Kumar, J. Singh, Synthesis of zinc substituted cobalt ferrites via reverse micelle technique involving in situ template formation: A study on their structural, magnetic, optical and catalytic properties, *Materials Chemistry and Physics*, 156 (2015), 188–197, doi:10.1016/j.matchemphys.2015.02.046
- D. M. Jnaneshwara, D. N. Avadhani, B. D. Prasad, Effect of zinc substitution on the nanocobalt ferrite powders for nanoelectronic devices, *Journal of Alloys and Compounds*, 587 (2014), 50–58, doi:10.1016/j.jallcom.2013.10.146
- A. Manikandan, L. J. Kennedy, M. Bououdina, J. J. Vijaya, Synthesis, optical and magnetic properties of pure and Co-doped ZnFe<sub>2</sub>O<sub>4</sub> nanoparticles by microwave combustion method, *Journal of Magnetism and Magnetic Materials*, 349 (2014), 249–258, doi:10.1016/j.jmmm.2013.09.013

- <sup>20</sup> S. Kumar, P. Kumar, V. Singh, Synthesis, characterization and magnetic properties of monodisperse Ni, Zn-ferrite nanocrystals, *Journal of Magnetism and Magnetic Materials*, 379 (2015), 50–57, doi:10.1016/j.jmmm.2014.12.006
- <sup>21</sup> J. M. Gao, Z. K. Yan, J. Liu, M. Zhang, Synthesis, structure and magnetic properties of Zn substituted Ni–Co–Mn–Mg ferrites, *Materials Letters*, 141 (2015), 122–124, doi:10.1016/j.matlet.2014.11.062
- <sup>22</sup> A. V. Raut, D. V. Kurmude, D. R. Shengule, Effect of gamma irradiation on the structural and magnetic properties of Co–Zn spinel ferrite nanoparticles, *Materials Research Bulletin*, 63 (2015), 123–128, doi:10.1016/j.jmmm.2015.09.013
- <sup>23</sup> J. Liang, H. R. Ma, W. Luo, S. L. Wang, Synthesis of magnetite submicrospheres with tunable size and superparamagnetism by a facile polyol process, *Materials Chemistry and Physics*, 139 (2013), 383–388, doi:10.1016/j.matchemphys.2012.10.027
- <sup>24</sup> I. Szczygiel, K. Winiarska, Synthesis and characterization of manganese–zinc ferrite obtained by thermal decomposition from organic precursors, *J. Therm. Anal. Calorim.*, 115 (2014), 471–477, doi:10.1007/s10973-013-3281-2
- <sup>25</sup> H. Huili, B. Grindi, G. Viau, Effect of cobalt substitution on the structure, electrical, and magnetic properties of nanocrystalline Ni<sub>0.5</sub>Zn<sub>0.5</sub>Fe<sub>2</sub>O<sub>4</sub> prepared by the polyol process, *Ceramics International*, 40 (2014), 16235–16244, doi:10.1016/j.ceramint.2014.07.059
- <sup>26</sup> R. Topkaya, A. Baykal, A. Demir, Yafet–Kittel-type magnetic order in Zn-substituted cobalt ferrite nanoparticles with uniaxial anisotropy, *J. Nanopart. Res.*, 15 (2013), 4–18, doi:10.1007/s11051-012-1359-6
- <sup>27</sup> R. S. Yadav, J. Havlica, M. Hnatko, Magnetic properties of Co<sub>1-x</sub>Zn<sub>x</sub>Fe<sub>2</sub>O<sub>4</sub> spinel ferrite nanoparticles synthesized by starch-assisted sol–gel autocombustion method and its ball milling, *Journal of Magnetism and Magnetic Materials*, 378 (2015), 190–199, doi:10.1016/j.jmmm.2014.11.027